catalysts

MDPI

Article

Hydrotreating of Waste Tire Pyrolysis Oil over Highly Dispersed Ni_2P Catalyst Supported on SBA-15

Gwang-Nam Yun [1], Ki-Duk Kim [2] and Yong-Kul Lee [3,*]

[1] Green Carbon Research Center, Korea Research Institute of Chemical Technology (KRICT), 141 Gajeongro, Yuseoung, Daejeon 34114, Korea; gnyun@krict.re.kr
[2] Climate Change Research Division, Korea Institute of Energy Research, 152 Gajeong-ro, Yuseong-gu, Daejeon 34129, Korea; kdkim87@kier.re.kr
[3] Laboratory of Advanced Catalysis for Energy and Environment, Department of Chemical Engineering, Dankook University, 126 Jukjeon, Yongin 448-701, Korea
* Correspondence: yolee@dankook.ac.kr

Abstract: A highly dispersed nickel phosphide catalyst supported on SBA-15 was prepared and tested for the hydrotreating of tire pyrolysis oil (TPO). Physicochemical properties of the prepared catalyst were analyzed by CO uptake chemisorption, BET, TEM, and X-ray diffraction (XRD). An advanced technique with gas chromatography equipped with mass spectrometry and atomic emission detector was applied to investigate carbon-, sulfur-, and nitrogen-containing compounds in TPO. Hydrotreating tests were carried out in a fixed-bed continuous flow reactor at 350 °C, 3.0 MPa, and LHSV of 0.5 h^{-1}. The Ni_2P/SBA-15 exhibited an HDS conversion of 89.3% and an HDN conversion of 60.7%, which was comparable to the performance of a commercial NiMoS catalyst under the same conditions.

Keywords: tire pyrolysis oil; Ni_2P catalyst; hydrotreating; HDS; HDN

Citation: Yun, G.-N.; Kim, K.-D.; Lee, Y.-K. Hydrotreating of Waste Tire Pyrolysis Oil over Highly Dispersed Ni_2P Catalyst Supported on SBA-15. *Catalysts* **2021**, *11*, 1272. https://doi.org/10.3390/catal11111272

Academic Editor: Jacques Charles Védrine

Received: 16 September 2021
Accepted: 19 October 2021
Published: 22 October 2021

1. Introduction

Global waste generation has grown steadily around the world, with 2 billion tons of municipal solid waste produced annually [1]. In particular, as concerns of massive waste tires rise, a chemical recycling technology for them has been extensively studied to overcome the environmental and economic issues [2,3]. Among the chemical recycling processes of waste tires, pyrolysis gives a high yield of oil, up to 38%, at moderate temperatures of around 500 °C [4,5]. The tire pyrolysis oil (TPO) has been regarded as a sustainable energy resource owing to a large amount of aromatics, olefins, and other substances, which can be used as valuable chemicals [6–8]. In particular, its high HHV (37–44 MJ/kg) led the way in the use of alternative fuels such as gasoline and diesel. However, TPO cannot be directly used as a fuel due to the high content of sulfur and nitrogen compounds derived from the synthesis processes of rubbers [3,8–10].

Catalytic hydrotreating is a promising process to produce usable liquid fuels with simultaneous eliminations of sulfur and nitrogen in the presence of H_2. Transition metal sulfide catalysts (NiMoS and CoMoS) have been commercially applied due to their hydrogenation ability in the hydrodesulfurization (HDS) and hydrodenitrogenation (HDN) processes [11–13]. Recently, numerous studies of transition metal phosphide catalysts have been considered as a potential candidate, showing high stability and resistance to aromatics and nitrogen-containing species [14–17]. However, metal phosphide catalysts have not yet been applied to the hydrotreating of TPO. Furthermore, although a number of studies for the hydrotreating of TPO have been reported [18–20], they did not provide a molecular-level qualitative analysis due to the complexity of TPO's components, which require high-performance analysis equipment.

In the present study, a highly dispersed nickel phosphide supported on SBA-15 was prepared, and its activity of TPO hydrotreating was investigated for the first time. The

activity was compared with a commercially available NiMoS catalyst, demonstrating Ni_2P as a potential catalyst for hydrotreating TPO. Furthermore, an advanced technique was applied to investigate the carbon-, sulfur-, and nitrogen-containing compounds in TPO and HYD products.

2. Results and Discussion

2.1. Characterizations of the Supported Nickel Phosphide Catalysts

Table 1 summarizes the physicochemical properties of the prepared samples. The BET surface areas of Ni_2P/SBA-15 and Ni_2P/SiO_2 were 687 and 124 $m^2\ g^{-1}$. After loading, the existence of metal phosphide and remaining phosphorus on the support led to a decrease in the surface area. The CO uptakes of Ni_2P/SBA-15 and Ni_2P/SiO_2 were 84.3 and 71.2 $\mu mol\ g^{-1}$.

Table 1. Physicochemical properties of supported Ni_2P catalysts.

Sample	BET Surface Area /$m^2\ g^{-1}$	CO Uptake /$mol\ g^{-1}$	Crystallite Size [a] /nm
SBA-15	687	-	-
Ni_2P/SBA-15	340	84.3	3.8
SiO_2(EH-5)	200	-	-
Ni_2P/SiO_2	124	71.2	9.1

[a] Crystallite size was calculated by Scherrer equation with 111 plane.

Figure 1 shows the XRD patterns of Ni_2P/SBA-15 and Ni_2P/SiO_2 catalysts. The broad feature centered at $2\theta = 22°$ is originated from amorphous silica. Both patterns show three main peaks at 40.5°, 44.8°, and 47.5°, corresponding to the characteristic peaks of hexagonal Ni_2P (space group: P .62m, D2 3 h, Struckturbericht notation: revised C22) [21]. The crystallite sizes were calculated by Scherrer's equation and presented sizes of 3.8 nm for Ni_2P/SBA-14 and 9.1 nm for Ni_2P/SiO_2, indicating that the Ni_2P particles on the SBA-15 support were more highly dispersed than those on the SiO_2 support.

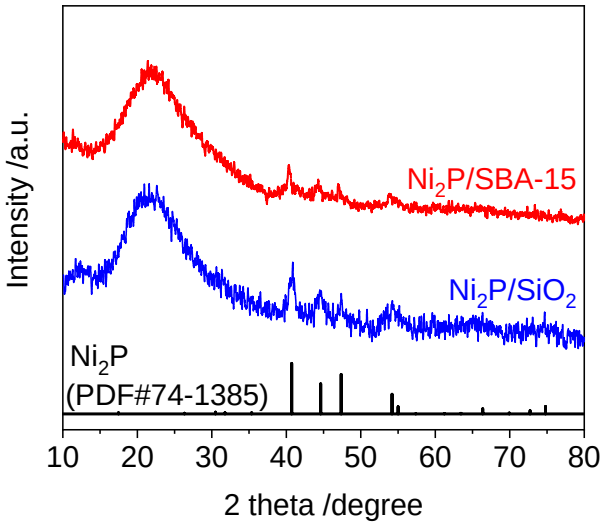

Figure 1. XRD patterns of Ni_2P/SBA-15 and Ni_2P/SiO_2 catalysts.

Figure 2 shows the TEM images and particle size distributions of Ni_2P/SBA-15 and Ni_2P/SiO_2 catalysts. The particle size distributions over 100 particles showed that the Ni_2P particles on SBA-15 had a narrow size distribution with an average size of around 5.3 nm, while the Ni_2P particles on SiO_2 had a broad size distribution with an average size

of around 9.7 nm. This result is in reasonable agreement with the crystallite sizes of Ni_2P determined by XRD in Figure 1.

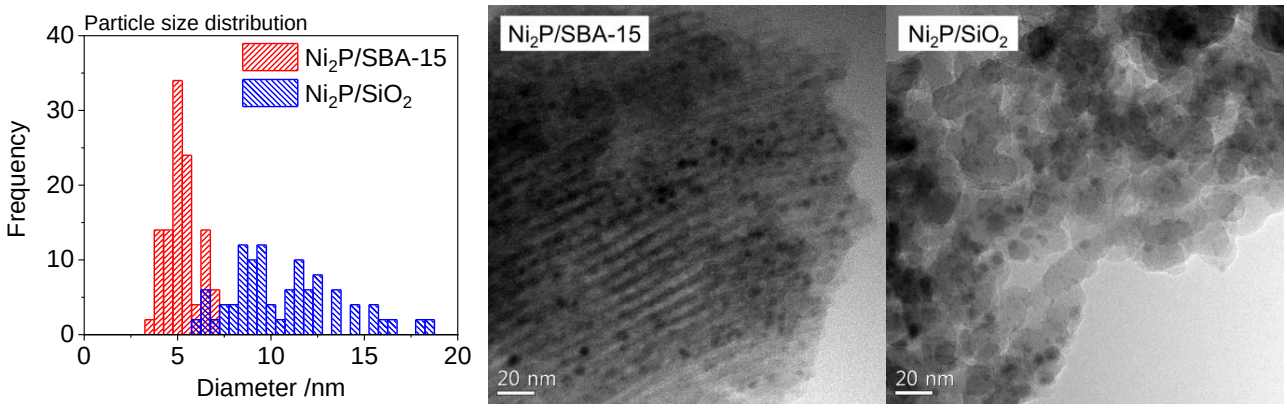

Figure 2. TEM images and particle size distributions of Ni_2P/SBA-15 and Ni_2P/SiO_2.

2.2. Characterizations of the Tire Pyrolysis Oil (TPO)

Tire pyrolysis oil (TPO) distilled at 320 °C was supplied from a refinery in the Republic of Korea. The specifications of the TPO used in this study are summarized in Table 2. The TPO contains 14,500 ppm of sulfur, 4070 ppm of nitrogen, and 41 wt.% of aromatic compounds (27 wt.% of mono-aromatics, 8 wt.% of di-aromatics, and 6 wt.% of tri+- aromatics).

Table 2. Composition and properties of tire pyrolysis oil (TPO).

Physical Properties		TPO
S/ppm		14,500
N/ppm		4070
Aromatics/wt.%	Total	41
	Mono	27
	Di	8
	Tri+	6
Distillation/°C	IBP/20/31	110/150/180
	44/58/72	210/240/270
	80/EP	290/320

To identify each heteroatom-containing compound of TPO, GC/AED (atomic emission detector) and GC/MS were used. In particular, GC/AED is a powerful technique in the analysis to assign the heteroatoms in complex oil mixtures because it selectively analyzes each element. The analyzed results of TPO and assigned compounds are demonstrated in Figure 3. The major compounds are benzene, toluene, xylene, and their derivatives. It is especially noteworthy that limonene is the most abundant compound in TPO. These results are compatible with previous reports [4,8], in which TPOs were observed to contain a significant amount of naphtha-like fractions along with about 15% limonene. Additionally, it is clear that the abundant sulfur-containing compounds of TPO are thiophene derivatives and benzothiazole, as shown in Figure 3b. In AED results of nitrogen-containing compounds (Figure 3b), the three major peaks were observed at the retention times of 7, 15, and 21 min, corresponding to aniline, benzothiazole, and dimethylquinoline, respectively. Note that the benzothiazole corresponded to both S- and N-selective analysis. It is reported that benzothiazole is derived from the vulcanizing accelerator in the form of benzothiazole derivatives [7,22]. It is a representative S and N compound for the hydrotreating of TPO [23].

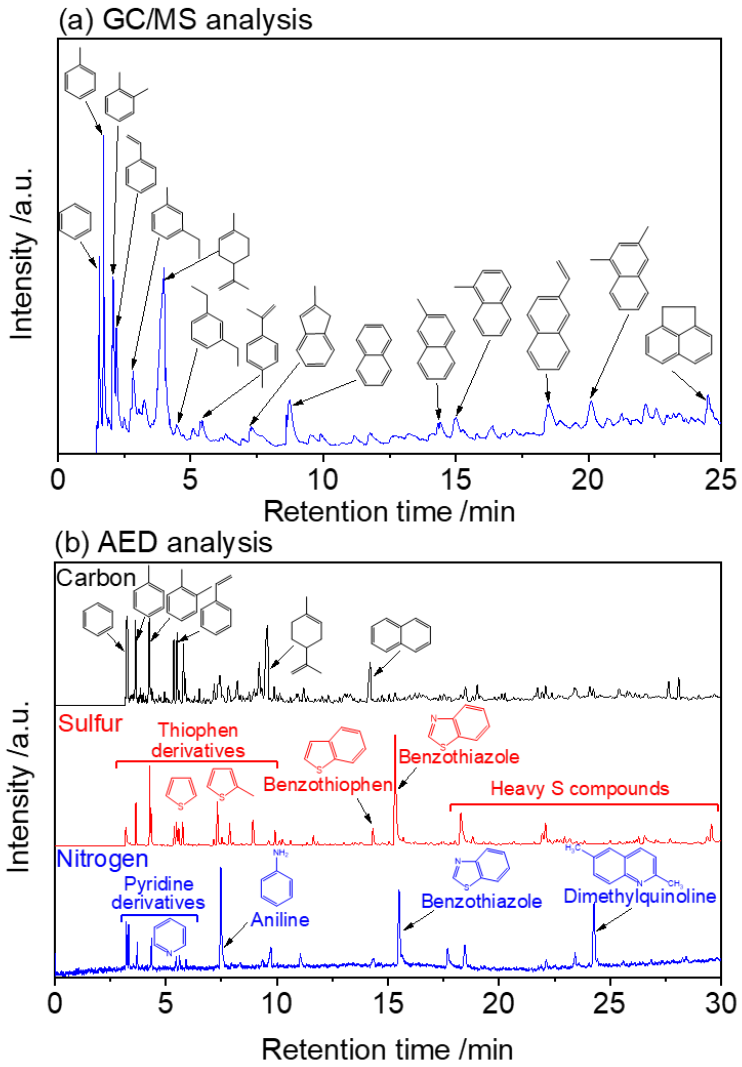

Figure 3. Characterization of tire pyrolysis oil by (**a**) GC/MS and (**b**) AED.

2.3. Activity Test

Figure 4 shows the AED chromatographs of hydrotreating products at 3.0 MPa, 350 °C, LHSV of 0.5 h^{-1}, and time on stream of 12 h on NiMoS, Ni_2P/SBA-15, and Ni_2P/SiO_2 catalysts. In the AED analysis of carbon-containing compounds (Figure 4a), the overall intensity of peaks was maintained after the hydrotreating process, but its products exhibited increased intensity in the peaks at 5–10 min, which are assigned as mono- or di-aromatics. These results indicate that the di- and tri-aromatics were converted to mono-aromatics. In the AED analysis of sulfur and nitrogen-containing compounds (Figure 4b), the hydrotreating products presented a substantial decrease in overall intensity compared to TPO. In the hydrotreating products, the peak assigned as benzothiazole was completely diminished, whereas the peaks at around 20–30 min were maintained. In the AED analysis of nitrogen-containing compounds (Figure 4c), the hydrotreating products displayed a substantial decrease in overall intensity compared to TPO. The peak assigned to benzothiazole was completely reduced, while those of aniline and dimethylquinoline remained.

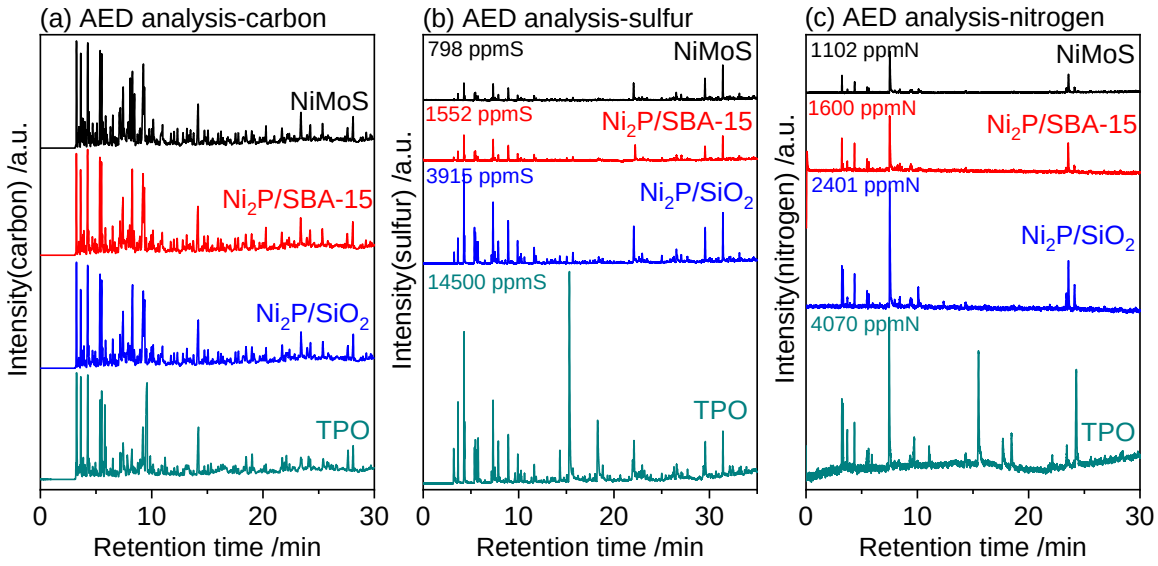

Figure 4. AED chromatographs of hydrotreating products on NiMoS, Ni_2P/SBA-15, and Ni_2P/SiO_2 catalysts at 3.0 MPa, 350 °C, LHSV of 0.5 h^{-1}, and time on stream of 12 h. (**a**) AED analysis-carbon, (**b**) AED analysis-sulfur, and (**c**) AED analysis-nitrogen.

Table 3 displays a comparison of reactivity of sulfur and nitrogen-containing compounds in TPO at 3.0 MPa, 350 °C, LHSV of 0.5 h^{-1}, and time on stream of 12 h on NiMoS, Ni_2P/SBA-15, and Ni_2P/SiO_2 catalysts. Total HDS and HDN conversions were obtained by the ASTM method, and the conversions of main sulfur and nitrogen compounds were calculated based on the AED intensity in Figure 4. The sulfur and nitrogen compounds were classified based on the retention time (light S and N (B.P. < 230 °C, R.T. < 15.3 min), benzothiazole (R.T. = 15.3 min), and heavy S and N (B.P. > 230, R.T. > 15.3 min)) and each conversion is summarized in Table 3. Additionally, the HDN conversions of three main N compounds (aniline, benzothiazole and dimethylquinoline) are listed in Table 3. The overall activities of HDS and HDN followed the order of NiMoS ≥ Ni_2P/SBA-15 > Ni_2P/SiO_2 at the applied conditions, and the commercial NiMoS catalyst exhibited the highest activity of around 94.5% total sulfur conversion, and 73% total nitrogen conversion. Furthermore, there is no significant change in the HDS and HDN conversion at the applied reaction conditions, as shown in Figure 5. The Ni_2P/SBA-15 showed comparable activity with commercial NiMoS, and higher activity than Ni_2P/SiO_2, suggesting that highly dispersed Ni_2P particles as confirmed by the results of CO uptakes, TEM, and XRD, led to the enhancement of the hydrotreating ability. This result can be explained by the structure of the Ni_2P catalyst that consists of two Ni sites, tetrahedral Ni(1) sites and square pyramidal Ni(2) sites. The latter sites responsible for the high catalytic activity in the hydrogenation are predominant in highly dispersed samples [24,25].

Table 3. Comparison of the reactivity of sulfur and nitrogen-containing compounds.

		NiMoS	Ni_2P/SBA-15	Ni_2P/SiO_2
HDS conversion/%	Total S	94.5	89.3	73.0
	Light S	90.8	82.5	57.4
	Benzothiazole	100	100	100
	Heavy S	47.9	79.9	43.0
HDN conversion/%	Total N	72.9	60.7	41.0
	Light N (Aniline)	78.4 (72.5)	63.8 (58.2)	70.2 (56.9)
	Benzothiazole	99.5	100	100
	Heavy N (Dimethylquinoline)	93.0 (84.3)	90.7 (84.3)	96.9 (93)

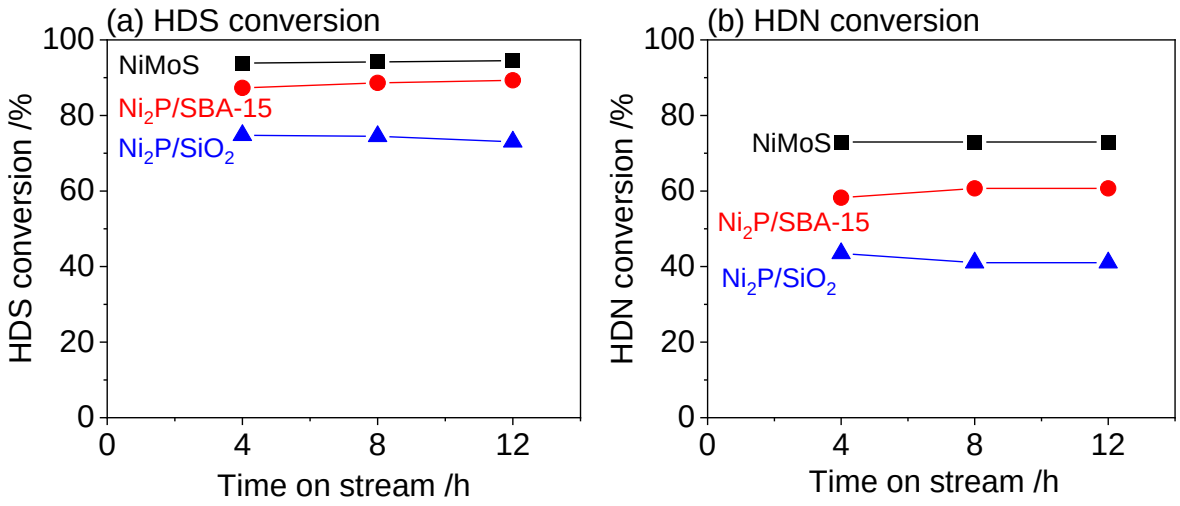

Figure 5. (**a**) HDS and (**b**) HDN conversion as a function of time on stream on NiMoS, Ni_2P/SBA-15, and Ni_2P/SiO_2 catalysts at 3.0 MPa, 350 °C, and LHSV of 0.5 h^{-1}.

In comparing reactivity in sulfur and nitrogen compounds, benzothiazole was the most reactive compound, with 100% conversion. This result is in accordance with previous work of hydrotreating scrap tire pyrolysis oil on NiMo catalysts [10]. They reported that benzothiazole was removed entirely, while substituted DBTs substantially remained in the hydrotreating products. As expected, light sulfur compounds such as thiophene derivatives showed higher reactivity than heavy sulfur compounds [26]. On the other hand, the nitrogen compounds had an opposite tendency compared to the light nitrogen compounds, including aniline, which showed the lowest reactivity among the nitrogen compounds. Thus, the reactivity of the main nitrogen compounds followed the order of benzothiazole > dimethylquinoline > aniline, suggesting that the basicity of the nitrogen compounds significantly affected their reactivity (benzothiazole = 2.5 pKa, aniline = 4.58 pKa and quinoline = 4.92 pKa). The nitrogen compounds with high basicity would be strongly adsorbed on the active sites and then limit the surface reaction, resulting in low reactivity. Apart from the basicity, it is presumable that aniline would be one of the intermediate products of benzothiazole, resulting in the low conversion of aniline.

Figure 6 shows the aromatic compound distributions of TPO and hydrotreating products, which were analyzed by high-pressure liquid chromatography with fluorescence detection (HPLC-FD). The TPO used in this study contains 41 wt.% of total aromatics consisting of 27, 8, and 6 wt.% of mono-, di-, and tri+-aromatics, respectively. NiMoS exhibited similar total aromatics, but a higher concentration of mono-aromatics and lower concentration of tri+-aromatics than those of TPO, indicating the transformation of poly-aromatics to mono-aromatics. The supported Ni_2P catalysts presented a substantial decrease in total aromatics and tri+-aromatic resulting from the full hydrogenation of aromatics to cycloalkane derivatives under the given reaction condition.

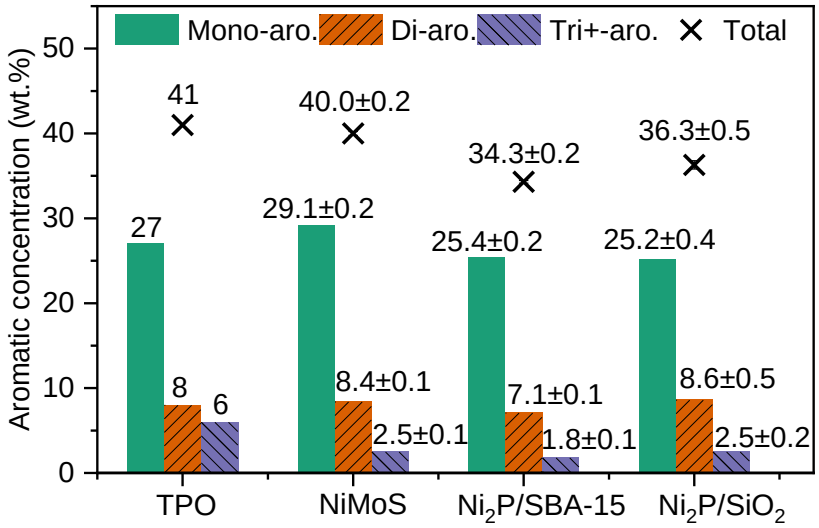

Figure 6. Aromatic compound distributions on NiMoS, Ni_2P/SBA-15 and Ni_2P/SiO_2 catalysts at 3.0MPa, 350 °C, LHSV of 0.5 h^{-1}, and time on stream of 12 h.

3. Experimental Section

3.1. Synthesis and Characterization of Supported Nickel Phosphide Catalysts

The supported nickel phosphide catalysts were synthesized by the incipient wetness impregnation method, as reported in [27]. The SiO_2(EH-5) was commercially obtained, and SBA-15 was prepared by the method reported in [17]. The impregnating solution was obtained by dissolving $Ni(NO_3)_2$ $6H_2O$ (Alfa Aesar, 98%) and $(NH_4)_2HPO_4$ (Samchun, 99%) in deionized water. The amount of nickel was 1.5 mmol per 1 g of support, and the initial Ni/P ratio was fixed at 1/2. The supported nickel phosphate precursor was dried at 120 °C overnight and then calcined in the air at 500 °C for 4 h. The resulting precursor was pelletized and sieved to a size of 650–1180 μm, followed by reduction at 600 °C for 2 h in H_2 flow (1000 mL min^{-1} per 1 g of sample). The temperature of reduction was determined by an H_2-TPR measurement, as reported previously [17]. After reduction, the sample was cooled in He and then passivated in 0.5% O_2/He flow at 25 °C for 4 h. A commercial NiMoS catalyst (TK-607 BRIM) was supplied as a comparison.

X-ray diffraction patterns (XRD) of the prepared phosphide catalysts were measured with a diffractometer (Bruker D8) operated at 40 kV and 100 mA, using a Cu-K_α monochromatic X-ray source. HR-TEM images were collected using a JEM-2100F, 200 kV microscope. Chemisorption uptakes of CO were measured by a pulse injection method using a re-reduced sample at 550 °C for 3 h in H_2 flow (100 mL min^{-1}). A Micromeritics ASAP 2010 micropore (Norcross, GA, USA) was used to measure the specific surface area of the passivated samples using N_2 adsorption isotherms at 77 K from the linear portion of BET plots (P/P_0 = 0.01–0.20).

3.2. Activity Test of Hydrotreating of Tire Pyrolysis-Oil (TPO)

The catalytic activity was tested in a fixed-bed continuous flow reactor at a 3.0 MPa, 350 °C, and liquid hour space velocity of 0.5–1.0 h^{-1}. Prior to the activity test, the passivated Ni_2P catalysts were re-reduced at 350 °C for 2 h under H_2 flow 100 cm^3 min^{-1}, and NiMoS catalyst was pretreated at 300 °C for 2 h under 100 cm^3 min^{-1} of 10% DMDS (dimethyl disulfide)/H_2. The tire pyrolysis oil was fed by means of a liquid pump along with hydrogen flow (100 cm^3 min^{-1}), and liquid products were collected at 4 h intervals. The total contents of sulfur and nitrogen in the liquid product were analyzed in an Antek 9000 NS analyzer using the combustion/fluorescence technique. Polycyclic aromatic hydrocarbons were monitored and quantified by high-pressure liquid chromatography with fluorescence detection (HPLC-FD). Total sulfur and nitrogen contents were analyzed in an Antek 9000 NS analyzer. A Hewlett-Packard gas chromatograph (HP6890) equipped

with an atomic emission detector (G2350A) was used to identify the carbon, sulfur, and nitrogen-containing compounds in TPO and hydrotreating products.

4. Conclusions

A highly dispersed nickel phosphide catalyst supported on SBA-15 was successfully prepared and tested for the hydrotreating (HYD) of tire pyrolysis oil (TPO). The activity tests reveal that Ni_2P/SBA-15 displayed comparable activity with commercial NiMoS catalyst and superior activity to Ni_2P/SiO_2 in HDS and HDN. Furthermore, it is noted that benzothiazole, which contains both sulfur and nitrogen, is the most reactive compound in TPO. A substantial decrease in tri+-aromatic hydrocarbons was observed in all catalysts. In particular, nickel phosphide catalysts exhibited superior hydrogenation activity for aromatic hydrocarbons. The analysis by GC-MS and AED demonstrated the carbon-, sulfur-, and nitrogen-containing compounds in TPO and hydrotreating products.

Overall results of catalytic activity gave an insight into the application of TPO in the field of chemical industry. The similarity of physical and chemical properties between hydrotreated TPO and commercial fuel oil would lead to its various practical applications in the petroleum industry. In particular, the finding of limonene as a major compound has the potential to expand the use of TPO.

Furthermore, the advanced analysis techniques provide a fundamental aspect in the hydrogenation of TPO. This can contribute to atomic-level catalyst design to enhance the selective conversion of a certain compound in TPO.

Author Contributions: Y.-K.L. conceived and designed the experiments; G.-N.Y. and K.-D.K. performed the experiments; G.-N.Y. and Y.-K.L. wrote the paper. All authors have read and agreed to the published version of the manuscript.

Funding: This research was funded by the National Research Foundation of Korea (NRF-2019R1A2C 2009999); the Ministry of Trade, Industry & Energy of Korea (MOTIE-10082582); and the University Innovation Support Program of Dankook University in 2021.

Data Availability Statement: The data presented in this study are available on request from the corresponding author.

Conflicts of Interest: The authors declare no conflict of interest. The funding sponsors had no role in the design of the study; in the collection, analyses, or interpretation of data; in the writing of the manuscript, and in the decision to publish the results.

References

1. Chen, D.M.C.; Bodirsky, B.L.; Krueger, T.; Mishra, A.; Popp, A. The world's growing municipal solid waste: Trends and impacts. *Environ. Res. Lett.* **2020**, *15*, 074021. [CrossRef]
2. Palos, R.; Gutiérrez, A.; Vela, F.J.; Olazar, M.; Arandes, J.M.; Bilbao, J. Waste Refinery: The Valorization of Waste Plastics and End-of-Life Tires in Refinery Units. A Review. *Energy Fuels* **2021**, *35*, 3529–3557. [CrossRef]
3. Gamboa, A.R.; Rocha, A.M.A.; dos Santos, L.R.; de Carvalho, J.A. Tire pyrolysis oil in Brazil: Potential production and quality of fuel. *Renew. Sustain. Energy Rev.* **2020**, *120*, 109614. [CrossRef]
4. Laresgoiti, M.F.; Caballero, B.M.; De Marco, I.; Torres, A.; Cabrero, M.A.; Chomón, M.J. Characterization of the liquid products obtained in tyre pyrolysis. *J. Anal. Appl. Pyrolysis* **2004**, *71*, 917–934. [CrossRef]
5. Williams, P.T.; Besler, S. Pyrolysis-thermogravimetric analysis of tyres and tyre components. *Fuel* **1995**, *74*, 1277–1283. [CrossRef]
6. Williams, P.T. Pyrolysis of waste tyres: A review. *Waste Manag.* **2013**, *33*, 1714–1728. [CrossRef] [PubMed]
7. Dos Santos, R.G.; Rocha, C.L.; Felipe, F.L.S.; Cezario, F.T.; Correia, P.J.; Rezaei-Gomari, S. Tire waste management: An overview from chemical compounding to the pyrolysis-derived fuels. *J. Mater. Cycles Waste Manag.* **2020**, *22*, 628–641. [CrossRef]
8. Cheng, Z.; Li, M.; Li, J.; Lin, F.; Ma, W.; Yan, B.; Chen, G. Transformation of nitrogen, sulfur and chlorine during waste tire pyrolysis. *J. Anal. Appl. Pyrolysis* **2020**, *153*, 104987. [CrossRef]
9. Mirmiran, S.; Pakdel, H.; Roy, C. Characterization of used tire vacuum pyrolysis oil: Nitrogenous compounds from the naphtha fraction. *J. Anal. Appl. Pyrolysis* **1992**, *22*, 205–215. [CrossRef]
10. Hita, I.; Gutiérrez, A.; Olazar, M.; Bilbao, J.; Arandes, J.M.; Castaño, P. Upgrading model compounds and Scrap Tires Pyrolysis Oil (STPO) on hydrotreating NiMo catalysts with tailored supports. *Fuel* **2015**, *145*, 158–169. [CrossRef]
11. Hwang, Y.-H.; Lee, Y.-K. Structure and activity of unsupported $NiWS_2$ catalysts for slurry phase hydrocracking of vacuum residue: XAFS studies. *J. Catal.* **2021**, in press. [CrossRef]

12. Dujardin, C.; Lélias, M.A.; van Gestel, J.; Travert, A.; Duchet, J.C.; Maugé, F. Towards the characterization of active phase of (Co)Mo sulfide catalysts under reaction conditions-Parallel between IR spectroscopy, HDS and HDN tests. *Appl. Catal. A* **2007**, *322*, 46–57. [CrossRef]
13. Ho, T.C. Deep HDS of diesel fuel: Chemistry and catalysis. *Catal. Today* **2004**, *98*, 3–18. [CrossRef]
14. Yun, G.N.; Ahn, S.J.; Takagaki, A.; Kikuchi, R.; Oyama, S.T. Hydrodeoxygenation of Γ-valerolactone on bimetallic NiMo phosphide catalysts. *J. Catal.* **2017**, *353*, 141–151. [CrossRef]
15. Yun, G.N.; Takagaki, A.; Kikuchi, R.; Ted Oyama, S. Hydrodeoxygenation of gamma-valerolactone on transition metal phosphide catalysts. *Catal. Sci. Technol.* **2017**, *7*, 281–292. [CrossRef]
16. Yun, G.N.; Cho, K.S.; Kim, Y.S.; Lee, Y.K. A new approach to deep desulfurization of light cycle oil over Ni_2P catalysts: Combined selective oxidation and hydrotreating. *Catalysts* **2018**, *8*, 102. [CrossRef]
17. Yun, G.-N.; Lee, Y.-K. Dispersion effects of Ni_2P catalysts on hydrotreating of light cycle oil. *Appl. Catal. B* **2014**, *150–151*, 647–655. [CrossRef]
18. Djandja, O.S.; Wang, Z.; Duan, P.; Wang, F.; Xu, Y. Hydrotreatment of pyrolysis oil from waste tire in tetralin for production of high-quality hydrocarbon rich fuel. *Fuel* **2021**, *285*, 119185. [CrossRef]
19. Han, Y.; Stankovikj, F.; Garcia-Perez, M. Co-hydrotreatment of tire pyrolysis oil and vegetable oil for the production of transportation fuels. *Fuel Process. Technol.* **2017**, *159*, 328–339. [CrossRef]
20. Dębek, C.; Walendziewski, J. Hydrorefining of oil from pyrolysis of whole tyres for passenger cars and vans. *Fuel* **2015**, *159*, 659–665. [CrossRef]
21. Rundqvist, S. X-Ray Investigations of Mn_3P, Mn_2P, and Ni_2P. *Acta Chem. Scand.* **1962**, *16*, 992–998. [CrossRef]
22. Pan, Y.; Yang, D.; Sun, K.; Wang, X.; Zhou, Y.; Huang, Q. Pyrolytic transformation behavior of hydrocarbons and heteroatom compounds of scrap tire volatiles. *Fuel* **2020**, *276*, 118095. [CrossRef]
23. Hita, I.; Aguayo, A.T.; Olazar, M.; Azkoiti, M.J.; Bilbao, J.; Arandes, J.M.; Castaño, P. Kinetic Modeling of the Hydrotreating and Hydrocracking Stages for Upgrading Scrap Tires Pyrolysis Oil (STPO) toward High-Quality Fuels. *Energy Fuels* **2015**, *29*, 7542–7553. [CrossRef]
24. Oyama, S.T.; Lee, Y.-K. The active site of nickel phosphide catalysts for the hydrodesulfurization of 4,6-DMDBT. *J. Catal.* **2008**, *258*, 393–400. [CrossRef]
25. Lee, Y.K.; Shu, Y.; Oyama, S.T. Active phase of a nickel phosphide (Ni_2P) catalyst supported on KUSY zeolite for the hydrodesulfurization of 4,6-DMDBT. *Appl. Catal. A* **2007**, *322*, 191–204. [CrossRef]
26. Kim, J.; Jang, J.G.; Lee, Y.K. Reactivity of sulfur compounds in FCC decant oils for hydrodesulfurization over $CoMoS_2/Al_2O_3$ catalysts. *Korean J. Chem. Eng.* **2021**, *38*, 1179–1187. [CrossRef]
27. Jang, J.-G.; Lee, Y.-K. Promotional effect of Ga for Ni_2P catalyst on hydrodesulfurization of 4,6-DMDBT. *Appl. Catal. B* **2019**, *250*, 181–188. [CrossRef]